MadAnalysis5 validation for the recasting of CMS-SUS-18-002: Supersymmetry search with photon, jets, b-jets and missing transverse momentum

Nukulsinh Parmar, Dr. Vinay Hegde, Dr. Seema Sharma

Indian Institute of Science Education and Research (IISER), Pune, India

emails: nukulsinh.parmar@students.iiserpune.ac.in, vinay.hegde@students.iiserpune.ac.in, seema@iiserpune.ac.in

Abstract

We present the MADANALYSIS5 implementation and validation of the CMS-SUS-18-002 analysis, which is a search for supersymmetry in events with photon, jets, b-jets and missing transverse momentum in proton-proton collisions at 13 TeV[1]. The data correspond to an integrated luminosity of $35.9\,fb^{-1}$ which were recorded by the CMS detector in 2016 at the CERN LHC. The recast code can be found on INSPIRE.

Contents

1 Introduction

The CMS-SUS-18-002 [1] is designed for the search for supersymmetry with photon, jets, b-jets and missing transverse momentum (MET). The results presented in CMS-SUS-18-002 are based on a dataset of proton-proton collisions recorded by CMS with a center-of-mass energy of 13 TeV and an integrated luminosity of $35.9\,fb^{-1}$. The analysis distinguishes signal-like events by categorizing the data into various signal regions based on the number of jets, the number of b-tagged jets, and missing transverse momentum.

The simplified models considered in the analysis are T5bbbbHg, T5bbbbZg, T5ttttZg and T6ttZg [1]. In the T5bbbbZg and T5ttttZg scenario, Fig. 1, each gluino decays to a pair of b quarks (or top quarks in case of T5ttttZg model) and a neutralino $\tilde{\chi}_1^0$ which decays to either a standard model Z and a gravitino $\tilde{G}$ or a photon and $\tilde{G}$. The branching ratio of $\tilde{\chi}_1^0 \to Z\tilde{G}$ and $\tilde{\chi}_1^0 \to \gamma\tilde{G}$ is assumed to be 50% each [1]. In T5bbbbHg model $\tilde{\chi}_1^0 \to H(\text{or } \gamma)\tilde{G}$. In T6ttZg model, the top squark decays into a top quark and a neutralino. The neutralino then decays to a γ/Z and a gravitino [1].

In the following, we have compared the predictions obtained with our MADANALYSIS 5 [2, 3, 4] reimplementation with the CMS results at every event selection and signal regions. The simplified model T5bbbbZg and T5ttttZg shown in fig 1 have been used as the benchmark signal scenario, and range of values of the masses of LSP and NLSP are considered.

2 Analysis Description

The CMS-SUS-18-002 analysis is designed for the search for supersymmetry with photon, jets, b-jets and missing transverse momentum. The analysis focuses on the hadronic decay of the top-antitop system and Z.
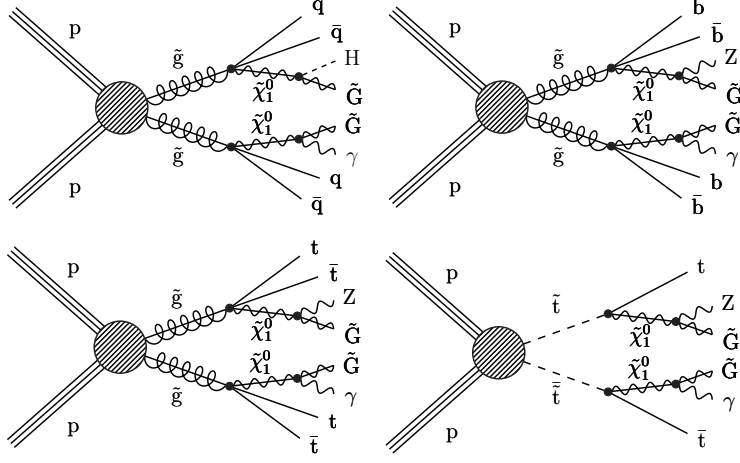
Figure 1: Figure 1: Feynman diagram of the simplified moedels - T5bbbbHg (top left), T5bbbbZg (top right), T5ttttZg (bottom left) and T6ttZg (bottom right)

2.1 Object definitions and preselection

These are the sequential selection applied to the events.

1. **Photon selection** :
   Photons with $p_T > 100 GeV$ and $|\eta| < 2.4$ are selected excluding the ECAL transition region $1.44 < |\eta| < 1.56$. The photon candidates are required to be isolated where isolation cone of radius $\Delta R = \sqrt{(\Delta\phi)^2 + (\Delta\eta)^2} < 0.3$ is used wiht no dependence on the p_T of the photon candidate. Also, the candidates matched to a track measured by the pixel detector (pixel seed) are rejected.

2. **lepton veto** :
   The selection of events requires no isolated leptons. The p_T of the lepton determines the isolation radius.

$$\Delta R = \begin{cases} 0.2 & \text{if } p_T < 50 \text{ GeV} \\ 10/p_T & \text{if } 50 \leq p_T \leq 200 \text{ GeV} \\ 0.05 & \text{if } p_T > 200 \text{ GeV} \end{cases}$$

   The isolation variable I is defined as

$$I = \frac{\sum_{<\Delta R} p_T(\text{charged hadrons}) + p_T(\text{neutral hadrons}) + p_T(\gamma)}{p_T(\text{lepton})}$$

   The isolation requirement is I<0.1 for electrons and I<0.2 for muons. After this isolation requirement, jets are cleaned [5] so that the overlap between the jet and leptons are removed from the jet collection.

3. **veto isolated tracks** :
   The selection of events required no isolated charged particle tracks. The isolation is defined as

$$I_i = \frac{1}{p_{T_i}} \sum_{j \neq i, \Delta R < 0.3}^{\text{all other charged particles}} p_{T_j}$$

   The cone of radius 0.3 is used. The isolation requirement is I < 0.2 if the track is electron or muon and I <0.1 otherwise. Isolated tracks are required to satisfy $|\eta| < 2.4$ and the transverse mass of each isolated track with $p_T^{miss}, m_T = \sqrt{2p_T^{track} p_T^{miss}(1 - cos\Delta\phi)}$ where $\Delta\phi$ is the difference in ϕ between $\mathbf{p}_T^{track}$ and $\mathbf{p}_T^{miss}$ is required to be less than 100 GeV.

4. **MET selection** :
   The selection of events requires the condition MET > 200 GeV. The defination of Missing Transverse Momentum (MET) is

$$\text{MET} = p_T^{miss} = |- \sum_{\text{visibile particles}} \mathbf{p}_T|$$

2

5. **Jets selection** :
   Jets are reconstructed by using the anti-kT [6] jet algorithm with a size parameter of 0.4. The selection of events requires atleast two jets in the event. Jets are required to have $p_T > 30$ GeV and $|\eta| < 2.4$. There is a difference in the value of size parameter in the standard MA5 delphes detector card, which is to be changed. The delphesMA5tune_card_CMS.tcl is provided in the documentation.

6. H_T^γ **and** p_T^γ **selection** : The signal-like candidate events are selected if they satisfy one of the following conditions -

   (a) $p_T^\gamma > 100$ GeV and $H_T^\gamma > 800$ GeV

   (b) $p_T^\gamma > 190$ GeV and $H_T^\gamma > 500$ GeV

7. $\Delta\phi$ **selection** :
   The signal-like events are selected if the conditions - $\Delta\phi(p_T^{miss}, \text{leading jet}) > 0.3$ and $\Delta\phi(p_T^{miss}, \text{second leading jet}) > 0.3$ are satisfied.

8. **b-jet selection** :
   Here this condition divides the signal like candidate events into to signal regions -

   (a) Nbjets $= 0$

   (b) Nbjets ≤ 1

   The identification of b jets in the paper [1] is performed by applying the combined secondary vertex algorithm (CSVv2) at the medium working point to the selected jet samples [7]. The signal efficiency for b jets with $p_T \sim 30 GeV$ is 55%. This b-tagging efficiency is the same as predefined in the delphesMA5tune_card_CMS.tcl card at the same working point.

2.2 Signal region selections

The analysis contains 25 independent signal regions based on p_T^{miss}, the number of jets N_{jets}, and number of b-tagged jets N_{b-jets}. The signal regions are grouped into 6 regions based on N_{jets} and N_{b-jets}. The N_{jets} is divided into 3 regions : 2-4, 5-6, ≤ 7, and the N_{b-jets} is divided into 2 regions : 0, ≤ 1. Now, these 6 regions are further divided into 4 regions based on p_T^{miss} : $200 < p_T^{miss} < 270, 270 < p_T^{miss} < 350, 350 < p_T^{miss} < 450, p_T^{miss} > 450 GeV$. In the lowest N_{jets} and N_{b-jets} region the highest p_T^{miss} bin is further subdivided such that the highest p_T^{miss} bin corresponds to $p_T^{miss} > 700 GeV$.

1. SR1 - $200 < p_T^{miss} \leq 270, 2 \leq N_{jets} \leq 4, N_{b-jets} = 0$

2. SR2 - $270 < p_T^{miss} \leq 350, 2 \leq N_{jets} \leq 4, N_{b-jets} = 0$

3. SR3 - $350 < p_T^{miss} \leq 450, 2 \leq N_{jets} \leq 4, N_{b-jets} = 0$

4. SR4 - $450 < p_T^{miss} \leq 700, 2 \leq N_{jets} \leq 4, N_{b-jets} = 0$

5. SR5 - $p_T^{miss} \geq 700, 2 \leq N_{jets} \leq 4, N_{b-jets} = 0$

6. SR6 - $200 < p_T^{miss} \leq 270, 5 \leq N_{jets} \leq 6, N_{b-jets} = 0$

7. SR7 - $270 < p_T^{miss} \leq 350, 5 \leq N_{jets} \leq 6, N_{b-jets} = 0$

8. SR8 - $350 < p_T^{miss} \leq 450, 5 \leq N_{jets} \leq 6, N_{b-jets} = 0$

9. SR9 - $p_T^{miss} \geq 450, 5 \leq N_{jets} \leq 6, N_{b-jets} = 0$

10. SR10 - $200 < p_T^{miss} \leq 270, N_{jets} \geq 7, N_{b-jets} = 0$

11. SR11 - $270 < p_T^{miss} \leq 350, N_{jets} \geq 7, N_{b-jets} = 0$

12. SR12 - $350 < p_T^{miss} \leq 450, N_{jets} \geq 7, N_{b-jets} = 0$

13. SR13 - $p_T^{miss} \geq 450, N_{jets} \geq 7, N_{b-jets} = 0$

14. SR14 - $200 < p_T^{miss} \leq 270, 2 \leq N_{jets} \leq 4, N_{b-jets} \geq 1$

15. SR15 - $270 < p_T^{miss} \leq 350, 2 \leq N_{jets} \leq 4, N_{b-jets} \geq 1$

16. SR16 - $350 < p_T^{miss} \leq 450, 2 \leq N_{jets} \leq 4, N_{b-jets} \geq 1$

17. SR17 - $p_T^{miss} \geq 450, 2 \leq N_{jets} \leq 4, N_{b-jets} \geq 1$

18. SR18 - $200 < p_T^{miss} \leq 270, 5 \leq N_{jets} \leq 6, N_{b-jets} \geq 1$

19. SR19 - $270 < p_T^{miss} \leq 350, 5 \leq N_{jets} \leq 6, N_{b-jets} \geq 1$

20. SR20 - $350 < p_T^{miss} \leq 450, 5 \leq N_{jets} \leq 6, N_{b-jets} \geq 1$

21. SR21 - $p_T^{miss} \geq 450, 5 \leq N_{jets} \leq 6, N_{b-jets} \geq 1$

22. SR22 - $200 < p_T^{miss} \leq 270, N_{jets} \geq 7, N_{b-jets} \geq 1$

23. SR23 - $270 < p_T^{miss} \leq 350, N_{jets} \geq 7, N_{b-jets} \geq 1$

24. SR24 - $350 < p_T^{miss} \leq 450, N_{jets} \geq 7, N_{b-jets} \geq 1$

25. SR25 - $p_T^{miss} \geq 450, N_{jets} \geq 7, N_{b-jets} \geq 1$

3 Event Generation

For our validation, we have two simplified models - T5bbbbZg and T5ttttZg. For T5bbbbZg model we have two sets of mass points $(m_{\tilde{g}}, m_{\tilde{\chi}_1^0}) = (1800, 150)$GeV and $(1800, 1750)$GeV and similarly for T5ttttZg we have $(m_{\tilde{g}}, m_{\tilde{\chi}_1^0}) = (1800, 150)$GeV and $(1800, 1550)$GeV.

The SUSY signal samples were produced using `MADGRAPH5_aMC@NLO` [8] for the hard scattering process and PYTHIA8 [9] was used for hadronization and showering. The supersymmetry model imported in the MADGRAPH5 was MSSM_SHLA2. Samples were generated with up to two additional parton. As pdg_Id of the $\tilde{G}$ is not defined in the given model, hence, in the parameter card of MADGRAPH, we have used pdg_Id of $\tilde{\chi}_1^0$ as $\tilde{G}$ with mass set at 1 GeV and pdg_Id of $\tilde{\chi}_2^0$ as $\tilde{\chi}_1^0$. The PYTHIA8 qcut parameter was set to 156 and the corresponding MADGRAPH5 xqut parameter is set to 30.

The CMS detector simulation was performed using the built in MA5 tuned Delphes3 [10]. Our detector simulation includes photon efficiencies provided on the public CMS webpage - https://twiki.cern.ch/twiki/bin/view/CMSPublic/SUSMoriond2017ObjectsEfficiency. Also, the pdg_Id of Gravitino is treated as an invisible particle during the simulation.

We have reweighted our events so that the total production rate for gluino pair production in proton-proton collisions at a center-of-mass energy of 13 TeV matches to the NLO+NLL cross sections taken from Ref [11].

$$\sigma(pp \to \tilde{g}\tilde{g})|_{\tilde{g}=1800GeV} = 0.00276 \text{ pb}$$

The event weight includes a normalization factor accounting of the integrated luminosity of 35.9fb^{-1}. Hence, the normalization is defined as -

$$N_\sigma = \frac{\sigma * \mathcal{L}}{\text{Number of events}} * 1000$$

4 Comparision with official results

The Table 1, 2 and 3 shows the comparisions between our predictions (MA5) and the official results provided by CMS. Table 1 and 2 are the cutflow for the baseline selection and Table 3 shows the signal region (SR) counts which are determined by applying the SR selection. Also, the graphical comparison of signal region counts between MA5 and CMS results is shown in fig 2.

We observe that the disagreement, on a cut-to-cut basis, is at most 25% before the N_{b-jets} cuts although, it is less than 15% in most of the cases. We use cut efficiency in order to compare the cutflow values. We have defined the efficiency of the cut as -

$$\text{Eff} = \frac{\text{no. of normalized events in the current cut}}{\text{no. of normalized events in the previous cut}} * 100$$

An additional ISR reweighting of events is done in the paper which we have not applied in our validation. This is one of the major reason for the large discrepency in the cut flow. The ISR reweighting will have more effect on discrepancy in the cases where mass difference between LSP and NLSP is less. Also it contributes to the uncertainty in the SR which ranges from 4% to 30% depending on the signal region and the signal parameters [1]. The SR comparison for T5bbbbZg (1800,1750) is better than the T5bbbbZg (1800,150). The uncertainties on the MA5 signal yield in the SR used in the Fig 2 does not include the effects of ISR reweighting while the CMS yields do include the effects of ISR reweighting. In the initial cut, there is a discrepancy between the MA5 and CMS values which should have been the same. The origin of this discrepancy is that the CMS analysis uses event filters which, has $\sim$ 98% - 99% efficiency. This filter efficiency is not applied to our implementation.

	T5bbbbZg			
	(1800, 150)		(1800, 1750)	
Selection	MA5 (Eff)	CMS (Eff)	MA5 (Eff)	CMS (Eff)
Initial	99.1 (xxxxx)	97.8 (xxxxx)	99.1 (xxxxx)	97.7 (xxxxx)
$p_T^\gamma > 100$GeV	41.0 (41.39%)	40.2 (41.10%)	56.7 (57.24%)	52.8 (54.04%)
veto e,μ	38.9 (94.86%)	37.2 (92.54%)	52.3 (92.20%)	47.4 (89.77%)
veto isolated tracks	38.1 (98.05%)	35.5 (95.43%)	50.4 (96.28%)	45.0 (94.94%)
$p_T^{miss} > 200$GeV	27.7 (72.71%)	26.0 (73.24%)	48.8 (96.97%)	43.0 (95.57%)
$N_jets \geq 2$	27.7 (100.0%)	26.0 (100.0%)	36.9 (75.57%)	33.4 (77.67%)
H_T^γ and p_T^γ selection	27.7 (100.0%)	26.0 (100.0%)	36.6 (100.0%)	33.2 (99.40%)
$\Delta\phi_1, \Delta\phi_2 > 0.3$	27.4 (87.90%)	23.0 (88.46%)	31.9 (87.31%)	29.5 (88.85%)
$N_{b-jets} = 0$	0.9 (3.54%)	1.6 (6.96%)	12.4 (38.45%)	12.3 (37.97%)
$N_{b-jets} \geq 1$	23.5 (96.46%)	21.3 (92.61%)	19.8 (61.55%)	19.7 (62.03%)

Table 1: Comparison of the cutflow predicted by MadAnalysis5 with official CMS cutflow for the Model T5bbbbZg

	T5ttttZg			
	(1800, 150)		(1800, 1550)	
Selection	MA5 (Eff)	CMS (Eff)	MA5 (Eff)	CMS (Eff)
Initial	99.1 (xxxxx)	97.6 (xxxxx)	99.1 (xxxxx)	97.9 (xxxxx)
$p_T^\gamma > 100$GeV	38.1 (38.47%)	37.0 (37.91%)	49.8 (50.25%)	45.4 (46.37%)
veto e,μ	15.7 (41.16%)	13.7 (37.03%)	21.5 (43.21%)	18.7 (41.19%)
veto isolated tracks	14.0 (89.40%)	11.4 (83.21%)	19.7 (91.42%)	16.5 (88.26%)
$p_T^{miss} > 200$GeV	10.5 (74.87%)	8.6 (75.44%)	18.9 (96.09%)	15.7 (95.15%)
$N_jets \geq 2$	10.5 (100.0%)	8.6 (100.0%)	18.8 (99.47%)	15.6 (99.36%)
H_T^γ and p_T^γ selection	10.5 (100.0%)	8.6 (100.0%)	18.8 (100.0%)	15.6 (100.0%)
$\Delta\phi_1, \Delta\phi_2 > 0.3$	9.4 (89.57%)	7.6 (88.37%)	16.4 (87.00%)	13.8 (88.46%)
$N_{b-jets} = 0$	0.30 (3.20%)	0.32 (4.21%)	3.2 (19.48%)	3.4 (24.63%)
$N_{b-jets} \geq 1$	9.1 (96.80%)	7.3 (96.05%)	13.2 (80.52%)	10.3 (74.64%)

Table 2: Comparison of the cutflow predicted by MadAnalysis5 with official CMS cutflow for the Model T5ttttZg

	T5bbbbZg (1800,150)		T5bbbbZg (1800,1750)	
Signal regions	MA5	CMS	MA5	CMS
SR1	0.024 ± 0.009	0.037 ± 0.008	0.352 ± 0.035	0.239 ± 0.050
SR2	0.024 ± 0.009	0.036 ± 0.008	0.338 ± 0.034	0.317 ± 0.055
SR3	0.034 ± 0.011	0.040 ± 0.009	0.608 ± 0.046	0.505 ± 0.085
SR4	0.051 ± 0.013	0.090 ± 0.018	2.296 ± 0.089	2.119 ± 0.345
SR5	0.041 ± 0.012	0.047 ± 0.010	7.350 ± 0.159	6.966 ± 1.119
SR6	0.075 ± 0.016	0.113 ± 0.023	0.041 ± 0.012	0.017 ± 0.006
SR7	0.089 ± 0.017	0.135 ± 0.028	0.044 ± 0.012	0.030 ± 0.009
SR8	0.095 ± 0.018	0.142 ± 0.029	0.031 ± 0.010	0.051 ± 0.014
SR9	0.188 ± 0.025	0.370 ± 0.075	1.097 ± 0.061	0.828 ± 0.209
SR10	0.038 ± 0.011	0.114 ± 0.027	0.010 ± 0.003	0.003 ± 0.002
SR11	0.068 ± 0.015	0.121 ± 0.029	0.003 ± 0.006	0.003 ± 0.002
SR12	0.038 ± 0.011	0.132 ± 0.032	0.010 ± 0.003	0.008 ± 0.003
SR13	0.092 ± 0.018	0.269 ± 0.064	0.113 ± 0.020	0.113 ± 0.042
SR14	0.419 ± 0.038	0.232 ± 0.031	0.410 ± 0.037	0.347 ± 0.067
SR15	0.450 ± 0.039	0.244 ± 0.033	0.492 ± 0.041	0.471 ± 0.074
SR16	0.481 ± 0.040	0.263 ± 0.034	0.834 ± 0.053	0.713 ± 0.107
SR17	1.534 ± 0.072	1.037 ± 0.106	13.802 ± 0.217	13.319 ± 1.905
SR18	1.773 ± 0.078	1.375 ± 0.166	0.085 ± 0.017	0.060 ± 0.019
SR19	1.913 ± 0.081	1.522 ± 0.183	0.106 ± 0.019	0.094 ± 0.026
SR20	1.892 ± 0.080	1.694 ± 0.205	0.164 ± 0.024	0.154 ± 0.040
SR21	4.320 ± 0.121	4.389 ± 0.508	3.000 ± 0.101	2.555 ± 0.614
SR22	2.063 ± 0.084	1.982 ± 0.340	0.021 ± 0.008	0.006 ± 0.004
SR23	2.250 ± 0.088	2.004 ± 0.345	0.017 ± 0.008	0.010 ± 0.005
SR24	2.257 ± 0.088	2.109 ± 0.365	0.031 ± 0.010	0.029 ± 0.012
SR25	4.153 ± 0.119	4.479 ± 0.761	0.697 ± 0.049	0.496 ± 0.180

Table 3: Yields in the signal region for the T5bbbbZg model with $(m_{\tilde{g}}, m_{\tilde{\chi}_1^0}) = (1800, 150), (1800, 1750)$GeV
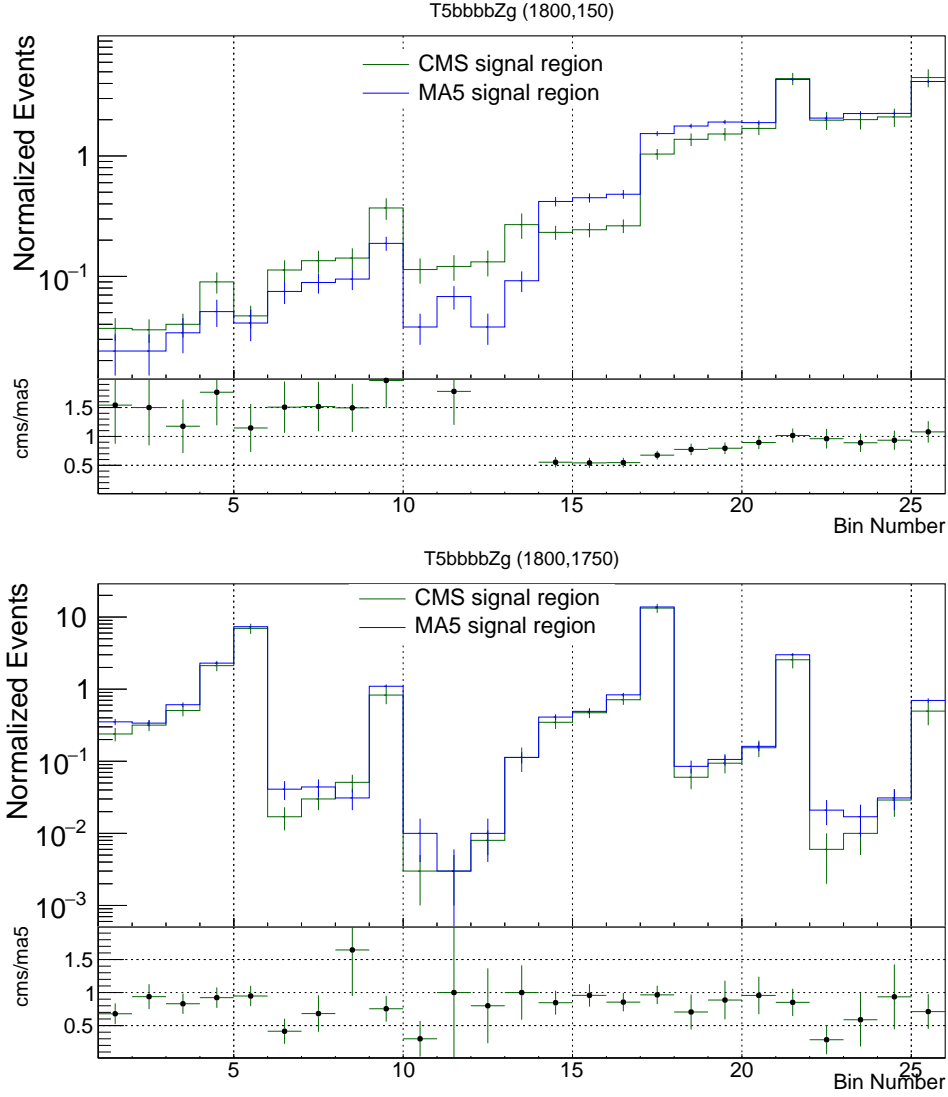
Figure 2: Figure 2: The SR yield comparsion between the MA5 and CMS for the models T5bbbbZg(1800,150) (top) and T5bbbbZg(1800,1750) (bottom).

5   Conclusion

We have presented the MADANALYSIS5 reimplementation of the CMS-SUS-18-002. All the pre-selection requirements have been incorporated and the signal events for a set of benchmark mass points have been used to validate the analysis implementation. The benchmark signal models used are T5bbbbZg and T5ttttZg. We have compared the cut flow and the signal regions of MA5 with official CMS values. The cut flow agrees within a deviation of about 25% without the application of ISR reweighting. The implementation is considered to be validated.
The reimplemented analysis code and the Delphes_MA5 tune cards are available on GITHUB -
https://github.com/Nukulparmar/MadAnalysis

6   Acknowledgement

I would like to thank Dr. Seema Sharma and Dr. Vinay Hegde for their constant help and interesting discussions for the project. I would also like to thank Raj Patil for helping me with event generation. I also thank KVPY for providing me the scholarship and the contingency grant for summer.

References

[1] A. M. Sirunyan *et al.*, "Search for supersymmetry in events with a photon, jets, b -jets, and missing transverse momentum in protonproton collisions at 13 TeV," *Eur. Phys. J.*, vol. C79, no. 5, p. 444, 2019.

[2] E. Conte, B. Fuks, and G. Serret, "MadAnalysis 5, A User-Friendly Framework for Collider Phenomenology," *Comput. Phys. Commun.*, vol. 184, pp. 222–256, 2013.

[3] E. Conte, B. Dumont, B. Fuks, and C. Wymant, "Designing and recasting LHC analyses with MadAnalysis 5," *Eur. Phys. J.*, vol. C74, no. 10, p. 3103, 2014.

[4] B. Dumont, B. Fuks, S. Kraml, S. Bein, G. Chalons, E. Conte, S. Kulkarni, D. Sengupta, and C. Wymant, "Toward a public analysis database for LHC new physics searches using MADANALYSIS 5," *Eur. Phys. J.*, vol. C75, no. 2, p. 56, 2015.

[5] F. Ambrogi and J. Sonneveld, "MadAnalysis5 recast of CMS-SUS-16-033," 2018.

[6] M. Cacciari, G. P. Salam, and G. Soyez, "The anti-k_t jet clustering algorithm," *JHEP*, vol. 04, p. 063, 2008.

[7] A. M. Sirunyan *et al.*, "Identification of heavy-flavour jets with the CMS detector in pp collisions at 13 TeV," *JINST*, vol. 13, no. 05, p. P05011, 2018.

[8] J. Alwall, R. Frederix, S. Frixione, V. Hirschi, F. Maltoni, O. Mattelaer, H. S. Shao, T. Stelzer, P. Torrielli, and M. Zaro, "The automated computation of tree-level and next-to-leading order differential cross sections, and their matching to parton shower simulations," *JHEP*, vol. 07, p. 079, 2014.

[9] T. Sjöstrand, S. Ask, J. R. Christiansen, R. Corke, N. Desai, P. Ilten, S. Mrenna, S. Prestel, C. O. Rasmussen, and P. Z. Skands, "An Introduction to PYTHIA 8.2," *Comput. Phys. Commun.*, vol. 191, pp. 159–177, 2015.

[10] J. de Favereau, C. Delaere, P. Demin, A. Giammanco, V. Lemaître, A. Mertens, and M. Selvaggi, "DELPHES 3, A modular framework for fast simulation of a generic collider experiment," *JHEP*, vol. 02, p. 057, 2014.

[11] W. Beenakker, S. Brensing, M. n. Kramer, A. Kulesza, E. Laenen, L. Motyka, and I. Niessen, "Squark and Gluino Hadroproduction," *Int. J. Mod. Phys.*, vol. A26, pp. 2637–2664, 2011.